Applied Surface Science 268 (2013) 472–476

Contents lists available at SciVerse ScienceDirect

Applied Surface Science

journal homepage: www.elsevier.com/locate/apsusc

Temperature and size effects on electrical properties and thermoelectric power of Bismuth Telluride thin films deposited by co-sputtering

Zhigang Zeng[a,b,*], Penghui Yang[a], Zhiyu Hu[a,b,*]

[a] Department of Physics, Shanghai University, Shanghai 200444, China
[b] Institute of NanoMicroEnergy, Shanghai University, Shanghai 200444, China

ARTICLE INFO

Article history:
Received 14 August 2012
Received in revised form
21 November 2012
Accepted 27 December 2012
Available online 5 January 2013

Keywords:
Bismuth telluride
Thermoelectric
Size effect
Electrical property

ABSTRACT

N-type Bismuth telluride thin films of different thicknesses were deposited on cleaned glass substrate at room temperature by co-sputtering technique. The films were annealed at 300 °C for 12 h in nitrogen atmosphere to improve their properties. The thermoelectric power and electrical properties measurements were carried out on the films with thickness from 70 nm to 480 nm in the temperature range 300–430 K. The thickness dependence of electrical resistivity and Seebeck coefficient of annealed films was analyzed using the effective mean free path model. Some physical parameters such as effective mean free path of charge carriers in hypothetical bulk, the exponent of the energy term of mean free path, activation energy, and the Fermi energy were calculated. Both the electrical conductivity and the Seebeck coefficient of the bismuth telluride films increased with increasing of film thickness and grain size. Films with fewer grain boundaries and defects have longer effective mean free path of carriers and the mean free path decreases with the increase of temperature. The electron–phonon interaction was considered as the main scattering mechanism in the annealed bismuth telluride thin films.

1. Introduction

Bismuth telluride (Bi_2Te_3) is known as one of the best thermoelectric materials with potential for a diverse range of applications, such as power generators [1], refrigerators [2], gas sensors [3]. It is a narrow band gap (0.15 eV [4]) semiconductor and exhibits a rhombohedral crystal structure. It is also known that bulk Bi_2Te_3-based materials have the highest thermoelectric figure of merit, $ZT \sim 1.14$ at room temperature [5]. The thermoelectric figure of merit is defined as $ZT = S^2\sigma T/\kappa$, where S [V K^{-1}] is the Seebeck coefficient, σ [S m^{-1}] is the electrical conductivity, T [K] is the absolute temperature, and κ [W m^{-1} k^{-1}] is the thermal conductivity, which has contributions from carriers and phonons [6]. Thus, it is important to improve thermoelectric figure of merit by increasing the thermopower $S^2\sigma$ and decreasing the thermal conductivity κ.

Current researches are focused on materials with nano-scale dimensions, such as thin films, quantum-dots superlattices, and nanowires, where manipulation of quantum confinement effects can further enhance thermoelectricity [7]. Low-dimensional structures may improve ZT drastically by confining electrons or holes in one or two dimensions [8]. Hicks and Dresselhaus predicted that ZT may be enhanced in a Bi_2Te_3 quantum well by a factor of ~13 over the bulk value [9]. In addition to its attractive thermoelectric properties, the band structure of Bi_2Te_3 makes it a promising candidate material for realization of a topological insulator [10,11], which is characterized by conductive states at the surface and insulating states in the bulk.

Several deposition techniques have been reported in the literatures for the fabrication of Bi_2Te_3 thin films: flash thermal evaporation [12], sputtering [13], electrochemical deposition [14], metal-organic chemical vapor deposition [15] and mechanically exfoliated method [16], are some examples. In this paper, the structural and electric characterization of bismuth telluride thin films deposited by co-sputtering was investigated. Thickness and temperature dependence of electrical resistivity and thermoelectric power of Bi_2Te_3 films were studied using the effective mean free path model of size-effect theory. From this analysis, important physical parameters have been deduced and they are reported in this paper.

2. Experiment

Bismuth telluride thin films were grown on cleaned glass substrate at room temperature from high-purity (4 N) Bi and Te target in a magnetron sputtering system (PVD75, Lesker). The background pressure was 3×10^{-6} mbar and the working pressure was 4×10^{-3} mbar. The RF sputtering power of Te and Bi was kept

* Corresponding authors. Tel.: +86 2166135201; fax: +86 2166135201.
E-mail addresses: zgzeng@shu.edu.cn, zeng.zigang@gmail.com (Z. Zeng), zhiyuhu@shu.edu.cn (Z. Hu).

0169-4332/$ – see front matter © 2013 Elsevier B.V. All rights reserved.
http://dx.doi.org/10.1016/j.apsusc.2012.12.134

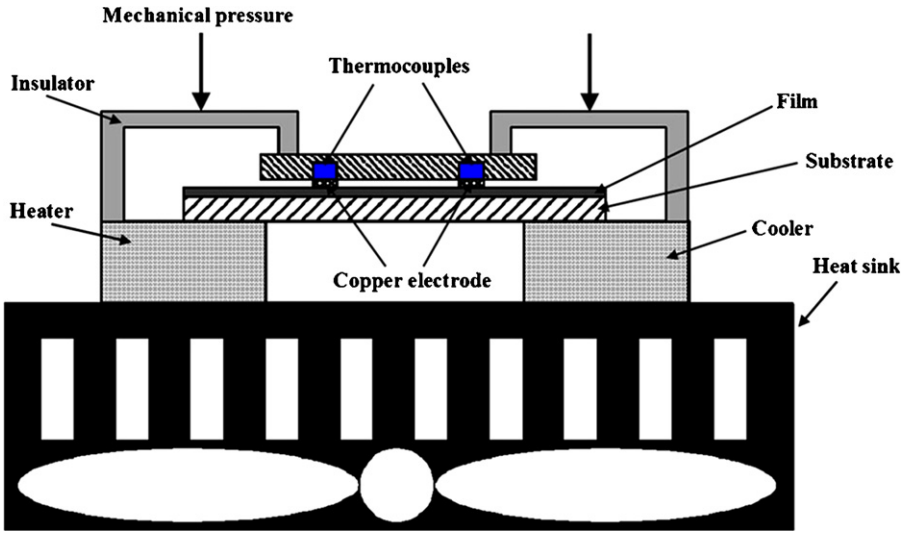

Fig. 1. Schematic of experimental set-up for Seebeck coefficient measurement.

constant at 22 W and 15 W, respectively, to ensure the films have stoichiometric Bi:Te ratio of ~2:3. After the deposition was complete, the films with thickness varying from 70 nm to 480 nm were then annealed at 300 °C for 12 h in N_2 atmosphere. The thickness of the films was determined using a surface profiler (XP-200, Ambios).

The microstructure of the films was studied by X-ray diffraction (XRD). XRD measurements were carried out in a DLMAX-2200 diffractometer using CuK_α radiation (λ = 0.154 nm). The morphology and composition were characterized using a scanning electron microscope (SEM, JSM-6700F) attached with Energy dispersive X-ray spectroscopy (EDS). The electrical properties of the films were determined using four probes technology. The Seebeck coefficients were obtained from the fit of linear of the measured Seebeck voltage versus the thermal gradient along the films. The Seebeck coefficient measurement system was homemade according to the method detailed in ref. [17]. The schematic of the experimental set-up are shown in Fig. 1. A temperature difference (<5 K) was built up for Seebeck coefficient measurement by putting a heater with a constant current controller under one side of a specimen. The distance between the thermocouple was 1 cm. A suitable mechanical pressure was applied to ensure good thermal and electrical contact. Each contact region between thermocouple with test film was 1 mm in diameter. An aluminum film (~100 nm) was evaporated on test films with mask to ensure ohmic contact. The thermoelectric power factor $S^2\sigma$ was calculated from the measured results of the electrical conductivity and the Seebeck coefficient.

3. Results and discussion

3.1. Structural analysis

XRD patterns of films with thickness of 360 nm using CuK_α radiation are shown in Fig. 2. The bismuth telluride films obviously has (0 1 5) preferred phase. After the films annealed at 300 °C for 12 h in N_2 atmosphere, the intensity of (0 1 5) and (1 0 1 0) peaks increased and the (0 0 6) phase showed up. It exhibits that prepared films have polycrystalline structure and that the annealing treatment helps the films eliminate defects and increase the degree of crystallinity. The grain size of the films with different thickness was obtained from the X-ray diffractogram peaks using the Scherrer formula $D = 0.9\lambda/\beta\cos\theta$, where D is the grain size, λ is the wavelength of the radiation used, β is the full width at half maximum and θ is the diffraction angle [18]. The values of grain size of films were calculated from preferred peak (0 1 5) and were listed in Table 1.

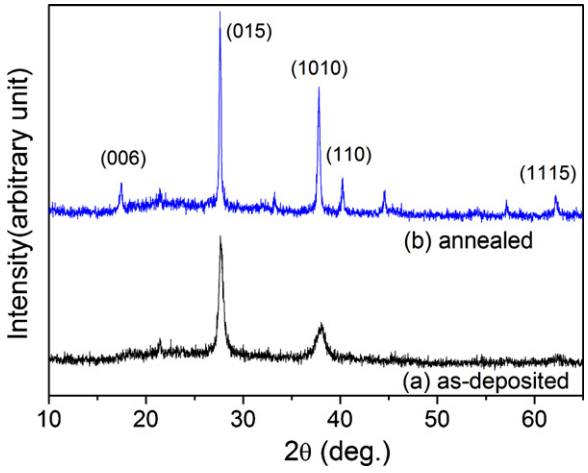

Fig. 2. X-ray diffraction spectra of (a) as-deposited and (b) annealed Bi_2Te_3 thin films with thickness of 360 nm.

It was found that the grain sizes of as-deposited films prepared by co-sputtering method had no obvious relationship with the thickness. However, the grain size of annealed films was larger than as-deposited films, and the value increased with increasing thickness of the film. This indicates that the micro-crystalline grains grow during annealing of the films and the grain size of annealed films is affected by the thickness of films.

The surface structure of the bismuth telluride thin films with thickness of 360 nm was investigated by SEM shown in Fig. 3. Both from surface and cross-section images, it clearly demonstrates that the annealed films have larger grains and more obvious grain boundaries. The composition of films was determined by ESD. The

Table 1
Variation of grain size and activation energy with thickness for Bi_2Te_3 thin films.

Thickness (nm)	Grain size (nm)/(0 1 5)		Activation energy (meV)
	As-deposited film	Annealed film	
70	14.6	21.1	42.6
130	17.3	34.1	38.6
260	18.4	40.4	33.3
360	17.9	45.9	27.7
470	18.9	53.4	–

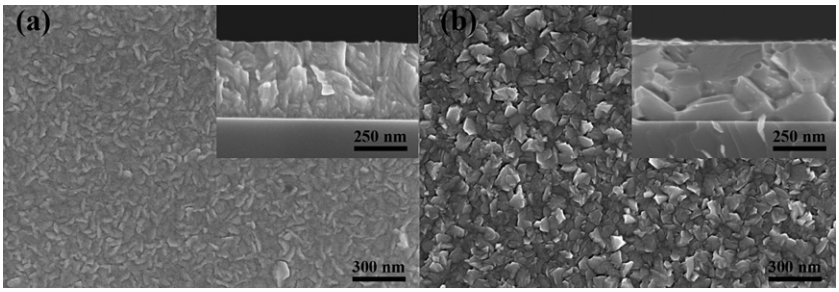

Fig. 3. SEM images of (a) as-deposited and (b) annealed Bi_2Te_3 thin films with thickness of 360 nm.

element content of Te in as-deposited films was ~63%, while in the annealed films was 61% which was slightly less than that in as-deposited films. This is caused by the re-evaporation of volatile element Te during the annealing process. However, the stoichiometric Bi:Te ratio of bismuth telluride films is confirmed nearly 2:3.

3.2. Temperature dependence of electrical properties

In order to study the temperature dependence of the conductivity of annealed films in more detail, the logarithmic variation of conductivity (σ) with inverse temperature ($1/T$) for annealed films is shown in Fig. 4. All the thin films exhibit almost linear behavior, indicating the semiconducting nature of the films. The conductivity increases with increasing of film thickness as well as the grain size. From the slope of the linear fit, the values of activation energy (listed in Table 1) for conduction in the films can be calculated according to the relation [18]:

$$\sigma = \sigma_0 \exp\left(-\frac{E_A}{k_B T}\right) \quad (1)$$

where σ_0 [S m^{-1}] is the temperature independent part of conductivity, E_A [J] is the conduction activation energy, k_B is the Boltzmann constant, and T [K] is the absolute temperature. It is found that the activation energy for conduction decreases as the thickness increases.

The variation of activation energy with thickness can be due to any one or a combined effects of the following causes: (i) variation in the grain size of the polycrystalline film, (ii) a large density of dislocations, (iii) quantum size effect and (iv) deviation of the stoichiometric Bi/Te ratio [19]. Since the film thickness and grain size is relatively large, the quantum size effect is neglectable. Careful growth technique followed by optimized annealing treatments would minimize the contributions due to dislocations and off stoichiometric compositions. The major contribution hence might be due to the size of the grains.

In general, there are a large number of grain boundaries in polycrystalline thin films, and the grain boundary consists of several atomic layers of disordered atoms which produce defects. Thus, when electrons move from one grain to another, more energy is needed for crossing the grain boundary. The electrical properties can be influenced by scattering of those disordered atoms, grain size and grain boundary density in polycrystalline films. Slater [20] proposed that the energy barrier was related with grain boundary and the activation energy could vary because of the charge accumulation at the boundaries. According to him, the variation is given as [20]:

$$E_A = E_0 + C(X - fD)^2 \quad (2)$$

where E_0 [J] is the original activation energy of single crystal supposed to be free of defects, C is a term depending on the density of charge carriers, electronic charge and dielectric constant of the material, X is the barrier width, D [m] is the dimension of the grain, and f is a fraction depending on the charge accumulation and the carrier concentration. Hence, the activation energy as function of grain size (shown in Fig. 5) demonstrates quadratic dependence on grain size according to the above expression. The solid line in Fig. 5 was well fitted by Eq. (2). It is found that the activation energy decreases with increasing of the grain size as expected. Therefore, the variation in activation energy can be primarily attributed to the changes of the grain size in the polycrystalline films.

3.3. Thickness dependence of electrical properties

3.3.1. Electrical resistivity

Films of different thicknesses ranging from 70 to 450 nm were prepared to study the effect of film thickness (t) on its electrical properties. The resistivity of annealed Bi_2Te_3 films was plotted against reciprocal thickness at different temperatures

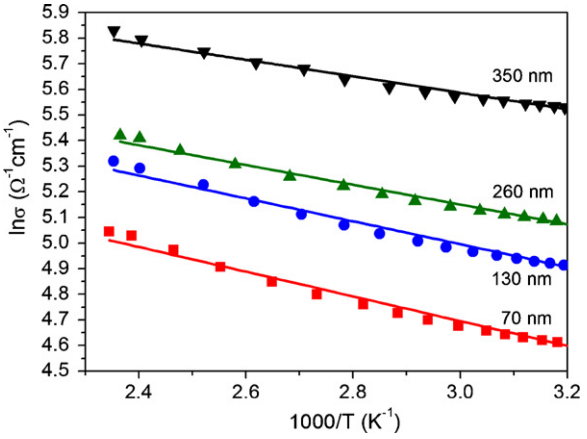

Fig. 4. Plots of lnσ versus $1/T$ for annealed films with different thicknesses.

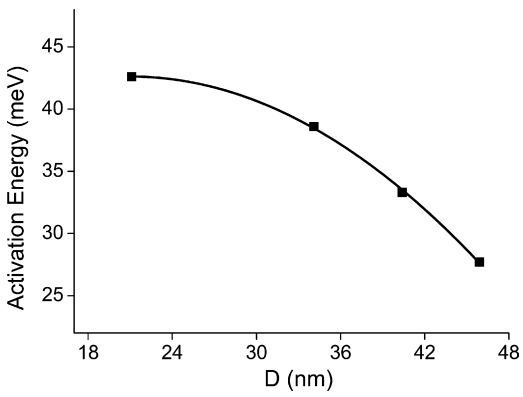

Fig. 5. Plot of activation energy versus the grain size.

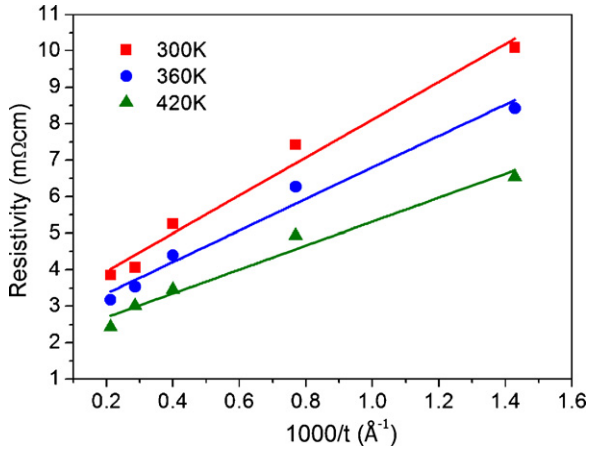

Fig. 6. Plots of resistivity versus the reciprocal thickness for annealed films at different temperature.

(Fig. 6) in order to obtain more details. It can be seen that the resistivity increases linearly with reciprocal thickness. Normally, surface and boundary scattering determine the electrical transport properties of polycrystalline films. When the thickness of the material becomes of the order of the mean free path, the classical size effect on the motion of charge carriers dominates. The thickness dependence of the films in the present study is explained on the basis of Tellier's model known as the effective mean free path model. According to this model, the resistivity of thin films (ρ_f) is given by [21]

$$\rho_f = \rho_b \left[1 + \frac{3}{8}\frac{\lambda_b}{t}(1-p)\right] \quad (3)$$

where ρ_b [Ω m] is resistivity of the infinitely thick polycrystalline film which has the same microstructure as that of films studied, λ_b [m] is effective mean free path of charge carriers in the hypothetical bulk, t [m] is the thickness and p is the specularity parameter which can vary between 0 and 1. The specularity parameter is an index to illustrate how charge carriers are scattered at the boundary surfaces. The case of $p = 1$ is valid for ideal single-crystalline films, which indicates that all the charge carriers are specularity scattered at the surface without any loss in the drift velocity component in the direction of the applied electric field. The case of $p = 0$ implies that the charge carriers are diffusely scattered with a complete loss in the direction of motion. It should be mentioned that p normally approaches 0 for polycrystalline films. Therefore, the value of p was assumed as 0 and 0.1 for the annealed films. Then, from the plot of ρ_f against $1/t$, ρ_b is given by the intercept and λ_b is calculated from the slopes. The calculated values of ρ_b and λ_b at different temperatures are listed in Table 2. It demonstrates that the resistivity of the infinitely thick polycrystalline film (ρ_b) and the mean free path (λ_b) decreases as the temperature increases due to increased lattice vibrations, as expected. The specularity parameter p has no effect on ρ_b, but λ_b can enlarge by increasing the value of p. It implies that the films with fewer grain boundaries and fewer defects in the crystalline grains can have longer effective mean free path of carriers.

Table 2
Physical parameters obtained according to Pichard models.

Temperature (K)	Resistivity ρ_b (m Ω cm)	Mean free path λ_b (nm)	
		$p = 0$	$p = 0.1$
300	3.03	455	506
360	2.82	387	430
420	2.38	266	296

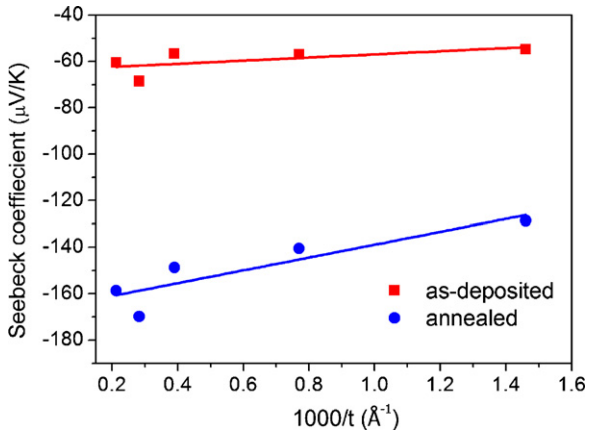

Fig. 7. Plots of Seebeck coefficient of films versus the reciprocal thickness.

3.3.2. Thermoelectric power

The Seebeck coefficient of films dependence of reciprocal thickness was described in Fig. 7. All the Seebeck coefficient values are negative, indicating that the as-deposited and annealed bismuth telluride films are n-type thermoelectric material. It is also clear that Seebeck coefficient of annealed films as well as as-deposited films increases with increasing of thickness. The quantum confinement effect on the electron density of states may lead to an increase in Seebeck coefficient of the films or nanowires in the scale below 10 nm [22]. Thus, there is no confinement effect in the prepared bismuth telluride films. The decrease in Seebeck coefficient with thickness may contribute to the increase in the carrier concentration, as the conductivity of films increases with thickness. However, the size effect on the Seebeck coefficient of annealed films displays much clearer than that of as-deposited films. The effective mean free path model developed by Tellier was extended by Pichard et al. [23] to calculate the Seebeck coefficient of polycrystalline films. According to this model, the expression for the Seebeck coefficient of a polycrystalline film (S_f) is given by [23]

$$S_f = S_b \left[1 - \frac{3}{8}\frac{\lambda_b}{t}(1-p)\frac{U}{1+U}\right] \quad (4)$$

where S_b [V K^{-1}] is the Seebeck coefficient of the infinitely thick polycrystalline film which has the same microstructure as that of films studied, and is given by [23]

$$S_b = -\frac{\pi^2 k_B^2 T}{3eE_F}(1+U) \quad (5)$$

where E_F is the Fermi energy, U is the exponent of the energy term of the hypothetical bulk mean free path, and is given by [23]

$$U = \left(\frac{\partial \ln \lambda_b}{\partial \ln E}\right)_{E=E_F} \quad (6)$$

Typically the exponent is 3/2 for impurity ion scattering, −1/2 for lattice acoustic scattering and zero for optical phonon scattering and so on.

According to the Eq. (4), the Seebeck coefficient of films would be linear relationship with reciprocal thickness. Hence, S_b was obtained from the intercept of the fitted lines (solid lines in Fig. 7) and $(1-p)\lambda_b U/(1+U)$ was calculated from the value of the slope. Then, the value of U was calculated using the λ_b value deduced from the thickness dependence plots of film resistivity. From the estimated values of S_b and U from the resistivity and thermoelectric power data analysis, the value of Fermi energy could be calculated from Eq. (5). As mentioned above, the value of p was assumed as 0 and 0.1 for the annealed films. However, the parameter of p can be eliminated during calculation. Then, the value of S_b, U, E_F is

Table 3
Physical parameters obtained according to Pichard models.

	S_b (μV K^{-1})	U	E_F (meV)
As-deposited films	−63.7	−0.298	81
Annealed films	−166.4	−0.089	40

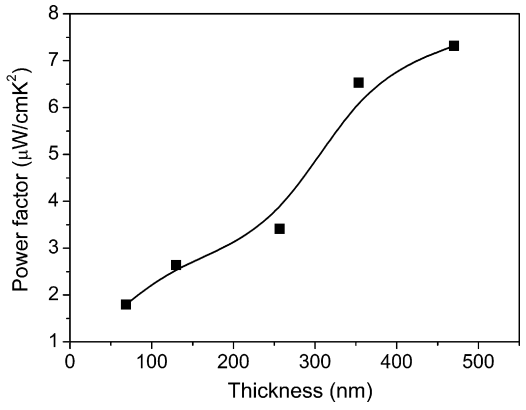

Fig. 8. Plot of thermoelectric power factor versus the annealed films thickness.

independent on p. Those physical parameters obtained according to Pichard model at room temperature are listed in Table 3. Since the annealing treatments are beneficial to elimination of defects, growth of grains and decrease in scattering, the S_b of annealed films is much larger than that of as-deposited films and the Fermi energy of annealed film is 40 meV which is half of the value of unannealed films. The negative value of the parameter U indicates that the electron-phonon interaction is the main scattering mechanism at room temperature in the bismuth telluride thin films [24] and the optical phonon scattering dominates in the annealed films.

The thermoelectric power factor $S^2\sigma$ was calculated from the measured thermoelectric power and electrical conductivity. The relationship between the power factor with thickness of thin film is shown in Fig. 8. It can be seen that $S^2\sigma$ is a function of thickness and is much lower than those reported for good bulk thermoelectric materials due to the size effect.

4. Conclusion

The bismuth telluride thin films with different thicknesses were prepared by co-sputtering technique to investigate the temperature and thickness effects on electrical properties and thermoelectric power. The films were annealed at 300 °C for 12 h in N_2 atmosphere. The grain size of annealed films was larger than as-deposited films, and the value increased with increasing thickness of the films. The temperature dependence of the conductivity of annealed films with different thicknesses was studied. The conductivity increases with increasing of film thickness as well as the grain size. The activation energy is found to be thickness dependent and it decreases with increasing thickness of the thin films. According to the Slater's model, the quadratic dependence of activation energy on the grain size indicates that the variation of activation energy primarily attributes to the changes of the grain size in the polycrystalline Bi_2Te_3 films. The thickness dependences of thermoelectric power and electrical resistivity are explained by the classical size effect theory based on the Tellier's model. Various physical parameters (λ_b, S_b, U, E_F) have been calculated using this model. The measured negative thermoelectric voltage for all thicknesses indicates n-type property of the films. Mean free path decreases with the increase of temperature, as expected. The negative value of the parameter U indicates that the electron–phonon interaction is the main scattering mechanism in the bismuth telluride thin films.

Acknowledgements

This research was supported by Shanghai Science and Technology Committee (10PJ1403800, 11DZ1111200, 12ZR1444000), Yunnan Provincial Science and Technology Department (2010AD003), National Natural Science Foundation of China (61204129), Innovation Foundation of Shanghai University and the Special Fund for Selection and Cultivation Excellent Youth in the University of Shanghai City.

References

[1] S. Bensaid, M. Brignone, A. Ziggiotti, S. Specchia, High efficiency thermoelectric power generator, International Journal of Hydrogen Energy 37 (2012) 1385–1398.
[2] J.P. Carmo, M.F. Silva, J.F. Ribeiro, R.F. Wolffenbuttel, P. Alpuim, J.G. Rocha, L.M. Goncalves, J.H. Correia, Digitally-controlled array of solid-state microcoolers for use in surgery, Microsystem Technologies 17 (2011) 1283–1291.
[3] K. Kalantar-Zadeh, W. Wlodarski, L. Li, S. Kandasamy, G. Rosengarten, A thermoelectric transducer based on bismuth telluride thin films for H_2 gas sensing, Journal of Rare Metal Materials and Engineering 35 (2006) 190–194.
[4] S.K. Mishra, S. Satpathy, O. Jepsen, Electronic structure and thermoelectric properties of bismuth telluride and bismuth selenide, Journal of Physics: Condensed Matter 9 (1997) 461–470.
[5] D. Tewldebrhan, V. Goyal, A.A. Balandin, Exfoliation and characterization of bismuth telluride atomic quintuples and quasi-two-dimensional crystals, Nano Letters 10 (2010) 1209–1218.
[6] A. Bulusu, D.G. Walker, Review of electronic transport models for thermoelectric materials, Superlattices and Microstructures 44 (2008) 1–36.
[7] A. Majumdar, Thermoelectricity in semiconductor nanostructures, Science 303 (2004) 777–778.
[8] M. Dresselhau, G. Dresselhaus, X. Sun, Z. Zhang, S. Cronin, T. Koga, Low-dimensional thermoelectric materials, Physics of the Solid State 41 (1999) 679–682.
[9] L.D. Hicks, M.S. Dresselhaus, Effect of quantum-well structures on the thermoelectric figure of merit, Physical Review B 47 (1993) 12727–12731.
[10] Y.L. Chen, J.G. Analytis, J.H. Chu, Z.K. Liu, S.K. Mo, X.L. Qi, et al., Experimental realization of a three-dimensional topological insulator, Bi_2Te_3, Science 325 (2009) 178–181.
[11] K.M.F. Shahil, M.Z. Hossain, D. Teweldebrhan, A.A. Balandin, Crystal symmetry breaking in few-quintuple Bi_2Te_3 films: applications in nanometrology of topological insulators, Applied Physics Letters 96 (2010) 153103.
[12] L.M. Goncalves, C. Couto, P. Alpuim, A.G. Rolo, F. Volklein, J.H. Correia, Optimization of thermoelectric properties on Bi_2Te_3 thin films deposited by thermal co-evaporation, Thin Solid Films 518 (2010) 2816–2821.
[13] D.H. Kim, E. Byon, G.H. Lee, S. Cho, Effect of deposition temperature on the structural and thermoelectric properties of bismuth telluride thin films grown by co-sputtering, Thin Solid Films 510 (2006) 148–153.
[14] S.H. Li, M.S. Toprak, H.M.A. Soliman, J. Zhou, M. Muhammed, D. Platzek, et al., Fabrication of nanostructured thermoelectric bismuth telluride thick films by electrochemical deposition, Chemistry of Materials 18 (2006) 3627–3633.
[15] A. Boulouz, A. Giani, F. Pascal-Delannoy, M. Boulouz, A. Foucaran, A. Boyer, Preparation and characterization of MOCVD bismuth telluride thin films, Journal of Crystal Growth 194 (1998) 336–341.
[16] V. Goyal, D. Teweldebrhan, A.A. Balandin, Mechanically-exfoliated stacks of thin films of Bi_2Te_3 topological insulators with enhanced thermoelectric performance, Applied Physics Letters 97 (2010) 133117.
[17] W. Helmut, K. Udo, H. Bernhard, W. Walter, Reliable measurement of Seebeck coefficient in semiconductors, Journal of Physics: Conference Series 176 (2009) 012037.
[18] V.D. Das, P.G. Ganesan, Electrical conduction studies on $(Bi_{0.6}Sb_{0.4})_2Te_3$ thin films, Semiconductor Science and Technology 12 (1997) 195–202.
[19] V.D. Das, P.G. Ganesan, Thickness and temperature effects on thermoelectric power and electrical resistivity of $(Bi_{0.25}Sb_{0.75})_2Te_3$ thin films, Materials Chemistry and Physics 57 (1998) 57–66.
[20] J.C. Slater, Barrier theory of the photoconductivity of lead sulfide, Physical Review 103 (1956) 1631–1644.
[21] C.R. Tellier, A theoretical description of grain boundary electron scattering by an effective mean free path, Thin Solid Films 51 (1978) 311–317.
[22] I. Bejenari, V. Kantser, A.A. Balandin, Thermoelectric properties of electrically gated bismuth telluride nanowires, Physical Review B 81 (2010) 075316.
[23] C.R. Pichard, C.R. Tellier, A.J. Tosser, Thermoelectric-power of thin polycrystalline metal-films in an effective mean free-path model, Journal of Physics F-Metal Physics 10 (1980) 2009–2014.
[24] C.R. Mallik, V.D. Das, Study of structural-, compositional-, and thickness-dependent thermoelectric and electrical properties of $Bi_{93}Sb_7$ alloy thin films, Journal of Applied Physics 98 (2005) 023710.